Solubility and Adhesion Characteristics of Plasma Polymerized Thin Films Derived from *Lavandula angustifolia* Essential Oil

Christopher D. Easton, Mohan V. Jacob

Electronic Materials Research Lab, School of Engineering and Physical Sciences, James Cook University, Townsville 4811, Australia

Received 9 March 2009; accepted 9 June 2009
DOI 10.1002/app.30916
Published online 1 September 2009 in Wiley InterScience (www.interscience.wiley.com).

ABSTRACT: Integration and implementation of organic polymer thin films often require knowledge of the stability when in contact with solvents and the adhesion quality when applied to different substrates. This article describes the solubility and adhesion characteristics of organic polymer thin films produced from *Lavandula angustifolia* essential oil, using radio frequency plasma polymerization at four RF power levels. Contact angle data was obtained for various solvents and used to determine the surface tension values for the polymer by using three established methods. A relatively strong electron–donor component and a negligible electronic acceptor component for the polymers indicate that they are monopolar in nature. Solubility data derived from interfacial tension values suggest that the polymers would resist solubilization from the solvents explored. The strongest solvophobic response was assigned to water, whereas diiodomethane demonstrated the weakest solvophobic response, with $\Delta G_{121} > 0$ in some instances depending on the surface tension values used. The adhesion tests of the polymers deposited on glass, PET, and PS indicated that the adhesion quality of the thin film improved with RF power, and it was associated with an improvement in interfacial bonding. © 2009 Wiley Periodicals, Inc. J Appl Polym Sci 115: 404–415, 2010

Key words: plasma polymerization; thin films; adhesion; solubility; contact angle

INTRODUCTION

Plasma polymerization has gained significant attention in recent years for the fabrication of polymer thin films and plasma modification of surfaces. This technique is a luminous chemical vapor deposition method that typically takes place in a low-temperature thermally nonequilibrium plasma. Polymer thin films produced through this method exhibit thickness homogeneity, physical and chemical stability, with smooth, pinhole free surfaces.[1,2] The properties of the polymers can be tuned by altering the deposition conditions, including RF power.[3] Such tuning can be used during deposition to induce effects, such as an optical gradient in the film.[4] Plasma polymers have been implemented in a number of applications involving electronics,[5] photonics,[6] and the biomedical[7,8] fields as protective coatings or functional thin films.

Polymer thin films fabricated from *Lavandula angustifolia* essential oil (LAEO)[9] and the resultant properties[10–12] have been reported previously. *L. angustifolia* is one of three major commercial species of the Spica group, from the genus *Lavandula*; the other two species from the Spica group are *Lavandula intermedia* and *Lavandula latifolia*.[13] LAEO contains more than 80 components, including a number of hydrocarbon-based components, in addition to metabolites that consist of ester, ketone, and ether groups. The major components of LAEO are linalool (approx. 23–57%) and linalyl acetate (approx. 4–35%).[14] Herein, the LAEO-based polymer films will be referred to as polyLA. These polymer films were derived from a nonsynthetic natural source that is environment friendly. The resultant polymer is primarily hydrocarbon based with oxygen-containing functional groups, including hydroxyl and ketone. PolyLA has the potential to be implemented in biomedical and optoelectronic applications.

The adhesion and solubility characteristics of a thin film coating are important when considering implementation of the polymer in many applications. The chosen application will determine the conditions that it is subjected to during its life span, including device fabrication. For example, the properties of a sacrificial material for use in air gap fabrication can be dependent on the intended application and processing restrictions. The required properties of a thermally degradable sacrificial material for use in the fabrication of nanofluidic channels can include

Correspondence to: M. V. Jacob (mohan.jacob@jcu.edu.au).

stability in solvents,[15] as acetone can be used to remove photoresist rather than using plasma ashing. However, within the microelectronics field, where air gaps are used to obtain structures with low dielectric constant, selective removal of a thermally degradable placeholder material can been performed without the use of wet etching.[16,17] In addition, sacrificial materials that are removed through wet etching rather than thermal processing have been used with the aim of lowering the total thermal budget of IC fabrication.[18,19] A previous study[12] has indicated that polyLA is a potential candidate for use as a sacrificial polymer, therefore knowledge of the adhesion and solubility characteristics are important for this and other potential applications.

The aim is to characterize the adhesion and solubility properties of polyLA produced through RF plasma polymerization. Contact angle (CA) measurement will be used to determine the interfacial tension and thus the solubility of the polymer in various solvents. Adhesion tests will be performed on films fabricated at the various input power levels and substrate types. Samples fabricated at RF power levels of 10, 25, 50, and 75 W will be compared to determine the deviation in these properties as a function of deposition parameters.

Theory

Solubility of the polymer in different solvents can be determined using surface tension components, using the procedure outlined by Wu and Shanks.[20] The solubility of solute 1 (the polymer) in solvent 2 (the solvent) can be derived from their interfacial tension (γ_{12}):[20,21]

$$\Delta G_{121} = -2\gamma_{12}, \tag{1}$$

where ΔG_{121} represents the free energy change. For $\Delta G_{121} >> 0$, solute 1 is solvophilic for solvent 2; $\Delta G_{121} << 0$, solute 1 is solvophobic for solvent 2; $\Delta G_{121} \approx 0$, solute 1 is partially dissolved in solvent 2.

To determine the interfacial tension for a polymer and solvent system, the surface tension of both parts is required. Wu and Shanks[20] used the surface tension component theory of Van Oss, Chaudhury, and Good (VCG) (also referred to as the Lifshitz-van der Waals/acid–base approach)[22] to obtain the surface tension values from CA measurements. However, there are several methods for obtaining surface tension values. The two main approaches are the VCG approach and the equation of state (EOS) approach (Ref. [23,24] and references therein).There is much debate concerning the use of such methods to find the surface energy and the most appropriate method to use. As such, there have been many publications addressing the validity of the methods,[24–28] accuracy,[29] and reviews of the available methods.[30,31] For this study, three approaches were chosen to provide a basis of comparison: the VCG approach, the EOS approach, and the Fowkes approach.[32]

VCG approach

The VCG approach involves considering the total surface tension of a surface as a sum of components. The γ^{LW} component is assigned to Lifshitz-van der Wall interactions, including dispersion, dipolar, and induction forces, and γ^{AB} is assigned to acid–base interactions, including electron donor–accepter interactions, such as hydrogen bonding.[20] The total surface tension for a substance i is thus given by:[33]

$$\gamma_i = \gamma_i^{LW} + \gamma_i^{AB} = \gamma_i^{LW} + 2\sqrt{\gamma_i^+ \gamma_i^-}, \tag{2}$$

where γ_i^+ represents the electron-acceptor parameters and γ_i^- the electron-donor parameter.

To determine the surface tension components for a solid, the following Young-Dupre equation for solid–liquid systems can be used:[22]

$$(1 + \cos\theta)\gamma_L = 2\left(\sqrt{\gamma_S^{LW}\,\gamma_L^{LW}} + \sqrt{\gamma_S^+\,\gamma_L^-} + \sqrt{\gamma_S^-\,\gamma_L^+}\right) \tag{3}$$

Therefore, using the known surface tension components for three liquids (L) and their corresponding CAs, the three surface tension parameters for the solid (S) can be determined. When choosing the three liquids to use, one should be a high-energy apolar liquid, such as diiodomethane, where γ_L^+ and γ_L^- are zero, and the remaining two should be polar liquids.[22]

EOS approach

This approach derives the surface tension from a purely thermodynamic point of view, and therefore neglects the molecular origins of surface tension. The following equation provides a method for calculating the surface energy of a solid from a single CA value (Ref. [23,24] and references therein):

$$\cos\theta_Y = -1 + 2\sqrt{\frac{\gamma_{sv}}{\gamma_{lv}}}e^{-\beta(\gamma_{lv}-\gamma_{sv})^2} \tag{4}$$

where the constant $\beta \approx 0.0001247$.[31]

Fowkes approach

Surface free energy of a solid can be calculated from the following equation:[31,32]

$$\left[\frac{1+\cos\theta}{2}\right] \times \left[\frac{\gamma_l}{\gamma_l^d}\right] = \sqrt{\gamma_s^p} \times \sqrt{\frac{\gamma_l^p}{\gamma_l^d}} + \sqrt{\gamma_s^d} \tag{5}$$

where γ^p is the polar component and γ^d the disperse component. It is recognized that γ^p can be replaced by γ^{AB}, and γ^d replaced by γ^{LW}. Using the procedure outlined by Deshmukh and Shetty,[31] interpreting eq. (5) as Y(LHS) = mX(RHS) + C and plotting LHS vs RHS for at least three solvents provides a straight line with a Y-axis intercept. The slope ($[\gamma^p]^{1/2}$) and intercept ($[\gamma^d]^{1/2}$) are used to determine the total surface energy.

Interfacial tension calculation

Once the surface tension values for the solid and liquid are known, the interfacial tension and thus the solubility can be determined. For a completely immiscible solid–liquid system, the interfacial tension is given by (Ref. [20] and references therein):

$$\gamma_{SL} = \gamma_S - \gamma_L \cos\theta \quad (6)$$

However, for a completely miscible system, the interfacial tension cannot be measured directly, although it can be obtained from the individual surface tension components based on the VCG approach (Ref. [20] and references therein):

$$\gamma_{12} = \left(\sqrt{\gamma_1^{LW}} - \sqrt{\gamma_2^{LW}}\right)^2 + 2\left(\sqrt{\gamma_1^+\gamma_1^-} + \sqrt{\gamma_2^+\gamma_2^-} - \sqrt{\gamma_1^+\gamma_2^-} - \sqrt{\gamma_1^-\gamma_2^+}\right) \quad (7)$$

Therefore, the use of eq. (7) is restricted to the surface tension components obtained using the VCG approach, however, eq. (6) can be applied using the value of surface tension for the solid obtained from any of the methods.

EXPERIMENTAL

L. angustifolia monomer obtained from G. R. Davis Pty Ltd was used in the fabrication of plasma polymer films using the experimental apparatus detailed previously.[9] The thin films were fabricated at a pressure of approximately 250 mTorr, and RF energy (13.56 MHz) was delivered to the deposition chamber via external copper electrodes separated by a distance of 11 cm. The deposition time was varied (2.5–12 min) in conjunction with the applied RF power (10–75 W) to produce films of approximately the same thickness. Approximately 1 mL of the monomer was placed into the holder for each successive deposition. The monomer inlet valve opened briefly to evacuate the holder before placing the substrate within the polymerization cell. During deposition, the monomer inlet was again opened and the vapor released into the chamber, where the flow rate was controlled via a vacuum stopcock. Three different types of substrate were used in this study: glass slides for the solubility and adhesion tests, and poly(ethylene terephthalate) (PET) and polystyrene (PS) (City Plastics Pty Ltd) for adhesion testing. Refer to ref[12] for substrate cleaning procedure.

CA measurements were performed using a KSV 101 system. The height of each drop was confirmed using a CCD camera before each measurement to ensure consistency in drop volume (8 μL). Six to eight drops were used to determine the average CA for each solvent–polymer combination. The solvents used in this study are listed in Table I. Once the drop was placed on the surface, the KSV CAM software was triggered to begin recording. An image was recorded every second for 30 s to monitor the CA as a function of time. CA values were derived from the raw data via image processing software by fitting the measured drop profile with the Young-Laplace equation.

Adhesion studies were performed using an Elcometer crosshatch tape adhesion test kit, complying with standard ASTM D3359. Similar adhesion studies have been performed previously on plasma polymers.[4,34] Using the cutting tool (6 teeth, 1 mm spacing), crosshatch patterns were made in the polymer films. Tape was then applied on top of the lattice followed by a pencil eraser across the surface to smooth out the tape. The tape was then removed by pulling at an angle of 180° and the results analyzed using a template of images to provide a qualitative value for adhesion. The adhesion was rated on a scale between 5 and 0, with 5 representing no delamination, 4 representing less than 5% delamination area, 3 representing 5– 15% delamination area, 2 representing 15–35% delamination area, 1 representing 35–65% delamination area, and 0 representing greater than 65% delamination area. Three samples were fabricated for each applied RF power and substrate combination, with three crosshatch tests performed on each sample, therefore a total of nine tests were performed for each applied RF power and substrate combination. Images of the tests were recorded using an optical microscope and CCD camera.

TABLE I
Solvents Used in Solubility Study

Solvent	Grade	Supplier
Ethylene Glycol (EG)	Laboratory	Ajax Finechem Pty Ltd
Glycerol	Analytical (99.5%)	Ajax Finechem Pty Ltd
Formamide	Laboratory (99.5%)	Ajax Finechem Pty Ltd
Dimethyl sulfoxide (DMSO)	Analytical (≥99.7%)	Ajax Finechem Pty Ltd
Diiodomethane (DIM)	≥98%	Merck Chemicals

RESULTS AND DISCUSSION

Contact angle

The KSV 101 system used in this study provided an equilibrium CA. The CA was measured at 1- s intervals to monitor any dynamic changes at the liquid–solid interface, including swelling or dissolution of the solid by the liquid.[24,35] As the measured CA has the potential to change as a function of time, these angles are then considered to be at instantaneous equilibrium with the surface and as such provide a representation of the surface state at each recorded point in time.[36]

As outlined previously,[10] the experimental procedure was confirmed by performing water CA measurements on PTFE. A linear fit was obtained from time-dependent data by using the equation $y = -0.01t + 119.95$ and $R^2 = 0.97$, where t represents time. Extrapolating to $t = 0$ gives a water CA for PTFE of 119.95° and was comparable to the result reported by Alexander and Duc ($y = -0.05t + 119$).[36]

CA data for the polyLA thin films fabricated at various power levels are presented in Figures 1–5, where the error bars represent the 95% confidence levels at each time interval. Table II contains the equation that provides the linear fit to each data set, where '*m*' also represents the rate of change of the CA, and '*c*' represents the extrapolated value for CA at $t = 0$ for each polymer and solvent combination. The water CA values have been reported previously[10] and are included to aid in determining the surface energy of the polymer.

The raw CA data present useful information concerning interactions between the surface and liquid system. An initial rapid decrease in the contact angle has been used to identify absorption of the solvent into the sample; furthermore, a relatively large rate of change in the contact angle has been attributed to reorientation of functionalities at the solid–liquid interface.[36] For example, the rate of change in CA reported by Alexander and Duc for water on PTFE (0.05° s^{-1}) was considered small enough to be negligible. Although the origin of this rate of change was not clarified by the authors, it was considered to be most likely occurring due to reactions between the solid–liquid interface, evaporation, or a combination of the two processes. Both these trends in the raw CA data provide an indication of the stability of the polymer while in contact with the applied solvents.

From the raw CD data for ethylene glycol (Fig. 1), an initial rapid drop in CA before stabilizing for all polymer samples was found, thus indicating absorption of the solvent into thin film. The rate of change of CA was relatively small (~0.005° s^{-1}), however, exhibited a positive gradient. Although this rate of change was considered insignificant, the positive gradient suggested the occurrence of reorientation of functionalities at the interface. For glycerol, there

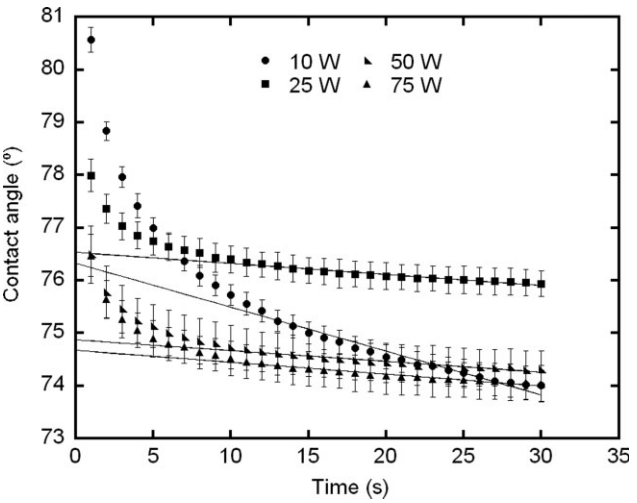

Figure 2 CA versus time for glycerol.

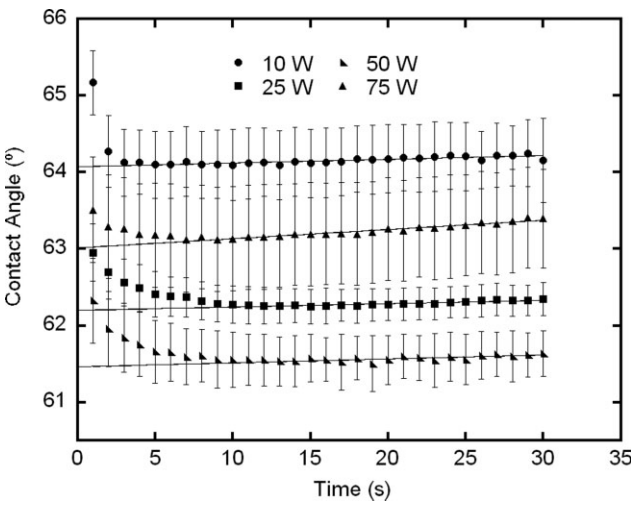

Figure 1 CA versus time for ethylene glycol.

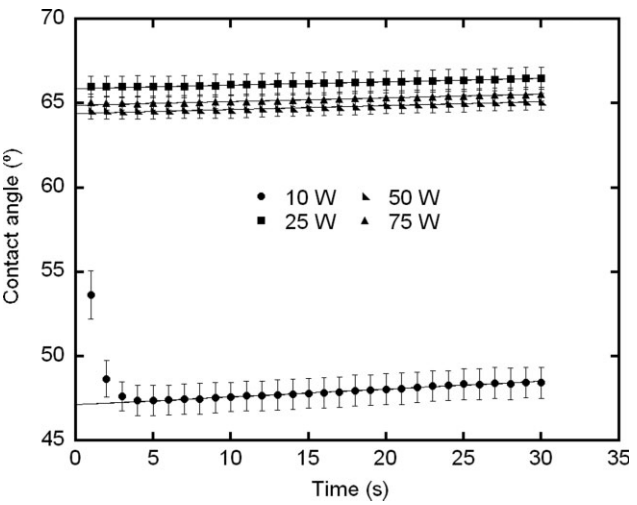

Figure 3 CA versus time for formamide.

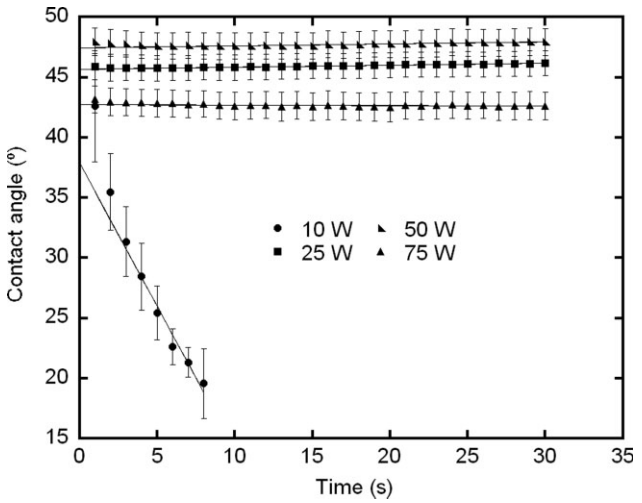

Figure 4 CA versus time for DMSO.

was also an initial rapid decrease of CA before stabilizing; however, the magnitude of the drop decreased with increased applied RF power during fabrication. A similar situation occurred with the formamide and DMSO data, where an initial rapid drop in CA occurs for the 10 W sample, although was not present for the other samples. Also for the DIM data, both the 10- and 25-W samples exhibited the initial rapid drop, whereas the 50- and 75-W data were relatively stable with time. These results indicated that the polymer was more stable as the RF power was increased, which was expected because an increase in RF power during fabrication typically results in an increase in crosslink density for this form of polymerization. It also signifies that the 10-W, and to a lesser extent the 25-W CA, data may not produce reliable surface energy results because of the significant error introduced by the rapid decrease.

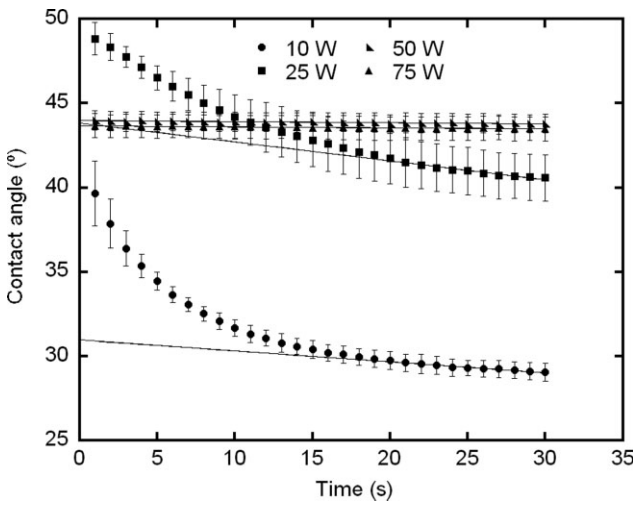

Figure 5 CA versus time for DIM.

TABLE II
Equations for Line of Best Fit and Corresponding CA Data for PolyLA Deposited at Four Rf Power Levels for the Solvents Examined

		Equation (mx + C)	
Liquid	Sample (W)	m/rate of change ($°s^{-1}$)	C/CA (°)
Water[10]	10	−0.0048	81.93
	25	−0.0062	83.64
	50	−0.0086	84.46
	75	−0.014	91.95
Ethylene glycol	10	0.0048	64.074
	25	0.0044	62.199
	50	0.0052	61.462
	75	0.0044	62.199
Glycerol	10	−0.0833	76.329
	25	−0.021	76.543
	50	−0.0204	74.877
	75	−0.0224	74.673
Formamide	10	0.0464	47.119
	25	0.0197	65.892
	50	0.0236	64.407
	75	0.0218	64.893
DMSO	10	−2.3732	37.848
	25	0.0161	45.692
	50	0.0157	47.469
	75	−0.004	42.73
DIM	10	−0.0645	30.965
	25	−0.1129	43.853
	50	−0.0063	43.981
	75	−0.0059	43.668

It was reported previously,[10] for the water CA measurements on polyLA, that an increase in the fabrication RF power resulted in an increase in the CA value and thus a decrease in the polarity of the polymer. The increase in CA was found to be the result of a decrease in the oxygen content of the resultant polymers, where the hydroxyl group diminished in intensity as RF power increased. Such a clear trend in the CA data was not present for the remaining solvents used in this study (Table II). This was most likely due to interactions occurring between the solvent–solid interface and was a further indication that the data sets for the lower RF power level samples may produce unreliable surface energy results.

Calculation of surface tension (surface energy)

Surface tension values for polyLA fabricated at different RF powers were calculated using the three methods outlined in the theory section. The contact angle data obtained for the solvents, together with the surface tension parameters, outlined in Table III were used in this study. The surface tension results from the VCG, EOS, and Fowkes approaches are presented in Tables IV, V, and VI, respectively, and the graphs used to determine the values for the Fowkes approach are shown in Figure 6.

TABLE III
Surface Tension Parameters for the Solvents Used

Solvent	γ	γ^{LW}	γ^{AB}	γ^+	γ^-
Water[a]	72.8	21.8	51.0	25.5	25.5
EG[b]	47.99	28.99	19.0	1.92	47.0
Glycerol[b]	64	34	30.0	3.92	57.4
Formamide[b]	57.49	38.49	19.0	2.28	39.6
DMSO[b]	43.58	35.58	8.0	0.5	32.0
DIM[a]	50.8	50.8	0	0	0
Hexane[c]	18.4	–	–	–	–
Chloroform[c]	27.32	–	–	–	–
Ethanol[c]	22.39	–	–	–	–
Acetone[c]	24.02	–	–	–	–

[a] Taken from ref. 18.
[b] Taken from ref. 24.
[c] Taken from. 37.

VCG approach

All possible solvent combinations involving one apolar liquid (DIM) and two polar liquids were used in the VCG approach to provide 10 iterations per sample. As predicted, some of the data obtained for the 10 W sample seems to contain significant error, with large negative values derived for some liquid combinations. However, not all of the surface tension data for the 10 W was affected.

From all the CA data obtained, the measurements for the solvent water[10] are the most stable, with no initial rapid drop in CA value, a small rate of change, and minor values for the 95% confidence limits. These results indicated that it was highly unlikely that any interactions are occurring between the surface–liquid interface and that the polymer was stable while in contact with water. Because of these favorable conditions, these CA values are expected to be accurate. Thus, it was not surprising that the stability in water CA values has transferred into the surface tension data calculated using the VCG approach. The surface tension components calculated using water as one of the solvents demonstrated the least variance when compared with the values calculated without the use of water. Therefore, emphasis will only be given to the surface tension values obtained using water as a solvent (see highlighted values in Table IV).

The γ^{LW} values calculated for the solid provide a benchmark for the lowest value of γ of a liquid that can be used to obtain CA values. In the case of the 10-W sample, $\gamma^{LW} = 43.82$, thus for a liquid, the lowest value of γ that can be successfully used in CA measurement is 43.82. In this study, DMSO has the lowest value of γ (43.58). As this value of γ was (slightly) smaller than the γ^{LW} value of the solid, the CA should not be measurable. As can be seen in Figure 4, the CA measurement for the 10-W sample demonstrates a rapid decrease with time, and in under 10 s becomes unmeasurable. For the remaining samples (25, 50, and 75 W), the CA data for DMSO was relatively stable and measurable. For these samples, $\gamma^{LW} \sim 37.63$ and thus was lower than the quoted value of γ for DMSO. Therefore, the raw CA vs. time data suggest that the calculated results of γ^{LW} were accurate.

Values for γ^+ and γ^- provide information concerning polar interactions with the surface. For this polymer, $\gamma^- >> \gamma^+$ and thus was considered monopolar. Most monopolar materials, however, are water soluble[20] as their value of γ^- are relatively large. It is possible to use this value of γ^- to determine an upper limit for which if exceeded, solubility will occur. Van Oss et. al.[21] demonstrated that for a γ^-

TABLE IV
Surface Tension Components Obtained for PolyLA Using VCG Approach

Sample	Liquid combination	γLW	$\gamma+$	$\gamma-$	γS
10 W	G:W:DIM	43.82	0.33	7.17	40.72
	EG:W:DIM	43.82	0.55	8.08	39.59
	F:W:DIM	43.82	0.72	1.56	45.94
	DMSO:W:DIM	43.82	0.16	6.24	41.82
	G:EG:DIM	43.82	1.34	24.00	32.47
	G:F:DIM	43.82	161.10	2313.50	−1177.10
	G:DMSO:DIM	43.82	0.08	2.33	42.97
	EG:F:DIM	43.82	52.00	1214.40	−458.80
	EG:DMSO:DIM	43.82	0.00	1.13	43.72
	F:DMSO:DIM	43.82	2.05	115.71	13.03
25 W	G:W:DIM	37.62	0.03	6.33	36.71
	EG:W:DIM	37.62	0.04	6.41	36.63
	F:W:DIM	37.62	0.05	6.57	36.45
	DMSO:W:DIM	37.62	0.06	6.67	36.34
	G:EG:DIM	37.62	0.06	7.44	36.33
	G:F:DIM	37.62	0.39	17.70	32.38
	G:DMSO:DIM	37.62	0.09	8.68	35.89
	EG:F:DIM	37.62	0.00	3.57	37.37
	EG:DMSO:DIM	37.62	0.10	9.70	35.66
	F:DMSO:DIM	37.62	0.07	7.35	36.19
50 W	G:W:DIM	37.55	0.00	4.94	37.63
	EG:W:DIM	37.55	0.01	5.54	37.01
	F:W:DIM	37.55	0.00	5.23	37.33
	DMSO:W:DIM	37.55	0.11	6.58	35.88
	G:EG:DIM	37.55	0.20	16.12	33.92
	G:F:DIM	37.55	0.36	20.95	32.07
	G:DMSO:DIM	37.55	0.31	19.57	32.61
	EG:F:DIM	37.55	0.15	13.67	34.69
	EG:DMSO:DIM	37.55	0.36	22.45	31.88
	F:DMSO:DIM	37.55	0.31	19.32	32.67
75 W	G:W:DIM	37.72	0.13	0.85	38.38
	EG:W:DIM	37.72	0.00	1.63	37.73
	F:W:DIM	37.72	0.04	1.20	38.13
	DMSO:W:DIM	37.72	0.00	1.52	37.84
	G:EG:DIM	37.72	0.79	32.41	27.63
	G:F:DIM	37.72	1.52	49.35	20.38
	G:DMSO:DIM	37.72	0.02	8.44	36.80
	EG:F:DIM	37.72	0.54	24.41	30.46
	EG:DMSO:DIM	37.72	0.01	0.59	37.89
	F:DMSO:DIM	37.72	0.00	4.58	37.45

W, water; EG, ethylene glycol; G, glycerol; F, formamide.

TABLE V
Surface Tension Values Obtained for PolyLA Using EOS Approach

	γs			
Solvent	10 W	25 W	50 W	75 W
Water	34.27	33.20	32.69	28.00
EG	27.52	28.39	28.74	28.01
Glycerol	31.72	31.60	32.55	32.67
Formamide	42.82	33.08	33.87	33.61
DMSO	35.47	32.42	31.70	33.60
DIM	44.28	38.96	38.90	39.04

W, water; EG, ethylene glycol; G, glycerol; F, formamide.

monopole surface (substance 1) and water, which is bipolar (substance 2), the following equation can provide that limit:

$$\gamma_{12}^{TOT} = \left(\sqrt{\gamma_1^{LW}} - \sqrt{\gamma_2^{LW}}\right)^2 + 2\left(\sqrt{\gamma_2^+\gamma_2^-} - \sqrt{\gamma_1^-\gamma_2^+}\right) \quad (8)$$

Using $\gamma_2^{LW} \approx 40$ mJ/m^2, it was found that eq. (8) becomes negative and thus the interfacial tension becomes negative for $\gamma_1^- > 28.31$ mJ/m^2. A negative interfacial tension between the material and water indicates that the water will tend to penetrate the material, leading to repulsion between the molecules or particles and promote solubilization.[21] As seen in Table IV, $\gamma^- < 28.31$ mJ/m^2 for all polymers, and thus indicates that they are not water soluble. It can also be seen that as the RF power was increased during deposition, the magnitude of γ^- tended to decrease, therefore providing another indicator that the hydrophobicity of the polymer increased with RF power.

EOS approach

For the EOS approach, the CA obtained for each solvent provides a unique result for the surface tension. There was some variance in the surface tension value between different solvents for each polymer (Table V). With the exception of the surface tension results from DIM, the values obtained using the EOS approach are smaller than those obtained with the VCG approach. Using the same assumption that was used for the VCG approach that the water CA values are the most accurate, then the values of surface tension derived using water should best represent the polymer. Therefore, the surface tension from the EOS approach for the polymer ranges from 34.27 to 28.00 mJ/m^2 for a RF power range of 10 to 75 W.

TABLE VI
Surface Tension Values Obtained for PolyLA Using the Fowkes Approach

γs			
10 W	25 W	50 W	75 W
39.66	33.93	34.26	36.61

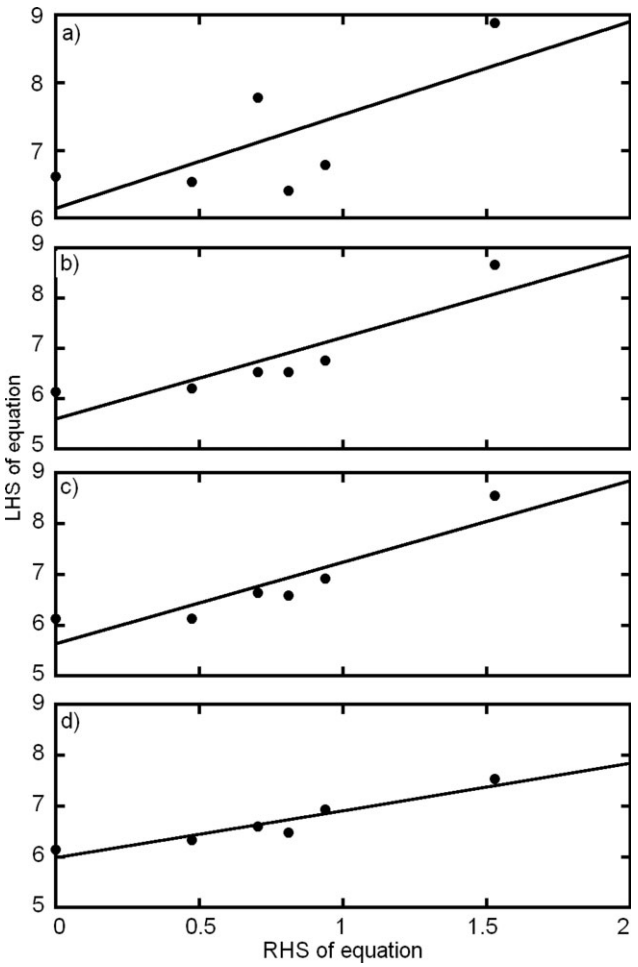

Figure 6 Graphs used to obtain surface tension values from the Fowkes approach using eq. (5) for samples (a) 10 W ($R^2 = 0.52$), (b) 25 W ($R^2 = 0.78$), (c) 50 W ($R^2 = 0.82$), and (d) 75 W ($R^2 = 0.90$).

Fowkes approach

All six contact angle values were used for each sample in the Fowkes approach to derive a single value of surface tension. From the plots used to derive the surface tension values (Fig. 6), it was apparent that the linear fit to the data improved with increasing RF power during deposition. Thus, this result demonstrated that the 10-W CA data contains a significant degree of error, and that the stability of the polymer while in contact with the solvents improved with increasing RF power. The results obtained with the Fowkes approach roughly compare with those obtained by the VCG and EOS methods. Overall, however, the results produced using the Fowkes and VCG methods are expected to be a more

TABLE VII
$\Delta G121$ Values Obtained for Each Solvent–Sample Combination Under Consideration Using eqs. (7) and (6) from the Derived Surface Tension Data

		Sample							
		10 W		25 W		50 W		75 W	
Solvent[a]	γ_s Data[b]	eq. (7)	eq. (6)	eq. (7)	eq. (6)	eq. (7)	eq. (6)	eq. (7)	eq. (6)
W	A	−50.07	−61.00	−53.71	−57.29	−61.36	−61.20	−81.76	−81.74
	B	−45.65	−58.74	−53.14	−57.13	−57.63	−59.96	−80.55	−80.44
	C	−71.48	−71.44	−52.29	−56.77	−60.06	−60.60	−81.05	−81.24
	D	−55.07	−63.20	−51.71	−56.55	−51.15	−57.70	−81.43	−80.66
	E		−48.10		−50.27		−51.32		−60.98
	F		−58.88		−51.73		−54.46		−78.20
EG	A	−16.61	−39.47	−22.17	−28.66	−26.78	−29.40	−25.48	−33.22
	B	−13.39	−37.21	−21.63	−28.50	−24.26	−28.16	−32.07	−31.92
	C	−15.10	−49.91	−21.07	−28.14	−26.43	−28.80	−28.47	−32.72
	D	−20.23	−41.67	−20.62	−27.92	−19.19	−25.90	−32.31	−32.14
	E		−26.57		−21.64		−19.52		−12.46
	F		−37.35		−23.10		−22.66		−29.68
G	A	−28.78	−51.19	−36.75	−43.60	−42.58	−41.87	−43.30	−42.92
	B	−24.69	−48.93	−36.10	−43.44	−39.45	−40.63	−50.08	−41.62
	C	−29.88	−61.63	−35.40	−43.08	−42.07	−41.27	−46.33	−42.42
	D	−33.34	−53.39	−34.84	−42.86	−33.21	−38.37	−50.43	−41.84
	E		−38.29		−36.58		−31.99		−22.16
	F		−49.07		−38.04		−35.13		−39.38
F	A	−13.87	−3.20	−20.21	−26.45	−24.60	−25.60	−24.70	−27.97
	B	−10.95	−0.94	−19.72	−26.29	−22.23	−24.36	−30.30	−26.67
	C	−13.69	−13.64	−19.20	−25.93	−24.21	−25.00	−27.24	−27.47
	D	−17.19	−5.40	−18.78	−25.71	−17.58	−22.10	−30.57	−26.89
	E		9.70		−19.43		−15.72		−7.21
	F		−1.08		−20.89		−18.86		−24.43
DMSO	A	−2.44	−12.62	−6.76	−12.54	−9.77	−16.34	−6.63	−12.74
	B	−0.47	−10.36	−6.40	−12.38	−8.07	−15.10	−12.45	−11.44
	C	1.64	−23.06	−6.04	−12.02	−9.58	−15.74	−9.32	−12.24
	D	−4.74	−14.82	−5.74	−11.80	−4.70	−12.84	−12.58	−11.66
	E		0.28		−5.52		−6.46		8.02
	F		−10.50		−6.98		−9.60		−9.20
DIM	A	−6.67	5.68	−3.72	−0.15	−2.00	−2.15	−3.27	−3.27
	B	−8.95	7.94	−4.00	0.01	−2.94	−0.91	−1.94	−1.97
	C	−4.75	−4.76	−4.27	0.37	−2.00	−1.55	−2.82	−2.77
	D	−4.51	3.48	−4.51	0.59	−5.40	1.35	−1.94	−2.19
	E		18.58		6.87		7.73		17.49
	F		7.80		5.41		4.59		0.27
Hex	A		−44.64		−36.62		−38.46		−39.96
	B		−42.38		−36.46		−37.22		−38.66
	C		−55.08		−36.10		−37.86		−39.46
	D		−46.84		−35.88		−34.96		−38.88
	E		−31.74		−29.60		−28.58		−19.20
	F		−42.52		−31.06		−31.72		−36.42
Chl	A		−26.80		−18.78		−20.62		−22.12
	B		−24.54		−18.62		−19.38		−20.82
	C		−37.24		−18.26		−20.02		−21.62
	D		−29.00		−18.04		−17.12		−21.04
	E		−13.90		−11.76		−10.74		−1.36
	F		−24.68		−13.22		−13.88		−18.58
Eth	A		−36.66		−28.64		−30.48		−31.98
	B		−34.40		−28.48		−29.24		−30.68
	C		−47.10		−28.12		−29.88		−31.48
	D		−38.86		−27.90		−26.98		−30.90
	E		−23.76		−21.62		−20.60		−11.22
	F		−34.54		−23.08		−23.74		−28.44
Ac	A		−33.40		−25.38		−27.22		−28.72
	B		−31.14		−25.22		−25.98		−27.42
	C		−43.84		−24.86		−26.62		−28.22
	D		−35.60		−24.64		−23.72		−27.64
	E		−20.50		−18.4		−17.34		−7.96
	F		−31.28		−19.8		−20.48		−25.18

[a] W, water; EG, ethylene glycol; G, glycerol; F, formamide; Hex, hexane; Chl, chloroform; Eth, ethanol; Ac, acetone.
[b] A, G:W:DIM (VCG); B, EG:W:DIM (VCG); C, F:W:DIM (VCG); D, DMSO:W:DIM (VCG); E, Water (EOS); F, Fowkes data.

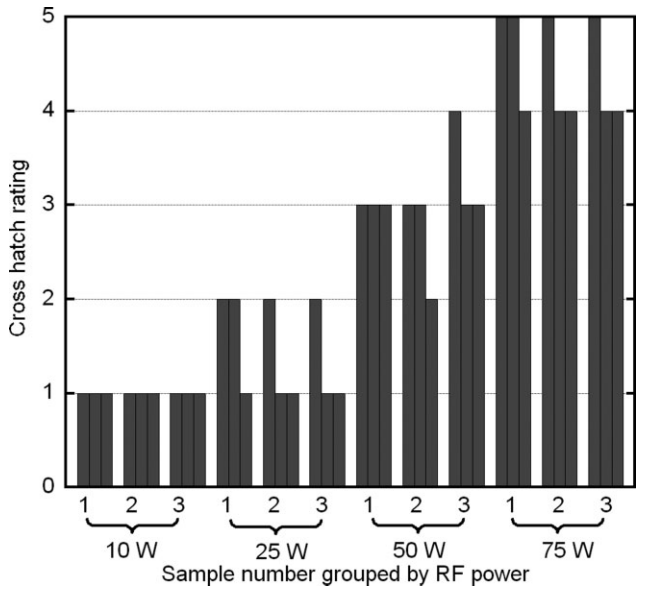

Figure 7 Adhesion data for polyLA deposited on glass at various RF power levels.

accurate representation of the polymer as they require more than one CA measurement to derive the surface tension values.

Calculation of solubility

The results of the solubility calculations using eqs. (6), (7) and (1) are presented in Table VII. ΔG_{121} values for the solvents used for CA measurement were calculated, as well as for some common solvents including hexane, chloroform, ethanol, and acetone. Because of the relatively low surface tension values for these solvents, it was not possible to obtain CA data and thus their CA was taken as 0°. In the instances where both eqs. (6) and (7) were used to obtain the interfacial tension for the solvent–solid system, in most cases the results were roughly equivalent, where the difference between the two values tended to decrease for increasing RF power.

ΔG_{121} values obtained suggest that the polymer would resist solubilization from the solvents examined. These results indicated that the strongest solvophobic response was assigned to water, which was expected as the CA values for water proved to be the most stable. ΔG_{121} derived for DIM demonstrated the weakest solvophobic response, with $\Delta G_{121} > 0$ for the results calculated using the EOS and Fowkes surface tension values.

Chloroform has been used to dissolve the polymer fabricated at 10 W to perform NRM spectroscopy,[10] however, dissolution of the polymer fabricated at higher power levels was not possible. Thus, there seems to be a contradiction between the calculated solvophobic response for the 10-W sample and experimental result. Results obtained at 10 W should then be considered a rough estimate at best. These results demonstrate the importance of determining CA values using solvents that are inert with the material under test. Interactions between the solvent and solid under test result in false CA values and thus an incorrect representation of the surface free energy of the solid.

The solubilization of the polymer in ethanol is important when considering implementing the film in biomedical applications. Ethanol was used previously to sterilize plasma polymers before implementation,[38] therefore the stability of the sample whilst immersed was necessary. The solubility data obtained indicated that the polymers would resist solubilization from ethanol and as such can be sterilized in this manner.

Adhesion study

The adhesion data obtained using the crosshatch test for polyLA deposited on glass, PET, and PS are presented in Figures 7–9, respectively. A general trend was observed for all three substrate types whereas the RF power during deposition was increased, the quality of the adhesion improved. In all cases, the 10-W samples demonstrated relatively poor adhesion, with the tape test removing a majority of the sample. The adhesion results for PET and PS were poor for the 25-W samples, however, a sharp improvement was observed for these substrates at 50 and 75 W. At the high RF powers, no delamination from the substrate was observed for PS, whereas minor (<5%) delamination was observed for a PET sample at 50 W and none at 75 W. An increase in adhesion quality was expected for

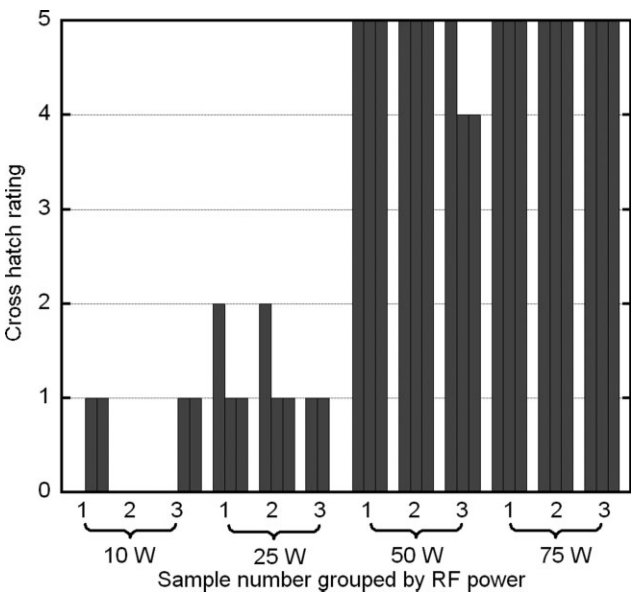

Figure 8 Adhesion data for polyLA deposited on PET at various RF power levels.

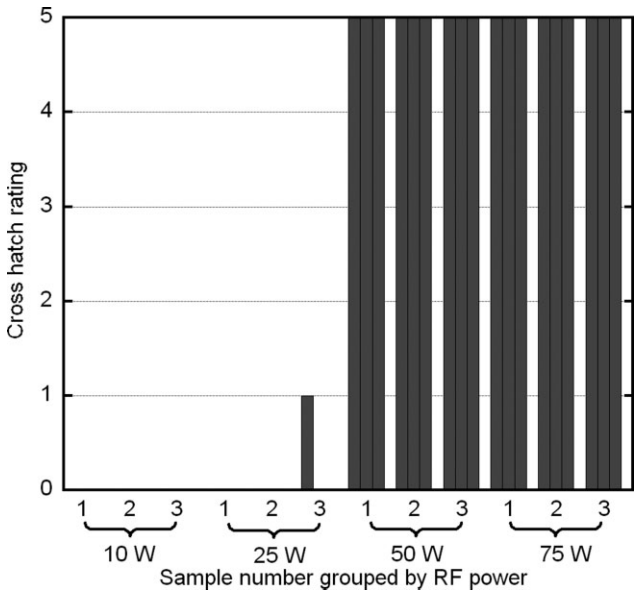

Figure 9 Adhesion data for polyLA deposited on PS at various RF power levels.

increasing RF powers, as an increase in energy input into a plasma and an associated increase in ion bombardment can improve interfacial bonding.[39] Examples of the adhesion results obtained using the optical microscope for PS (Fig. 10), glass (Fig. 11), and PET (Fig. 12) are presented.

Although the adhesion results of the polymer films fabricated at high RF power demonstrated good adhesive properties, at low RF power further improvement is possible. It is known that plasma-assisted surface modification of substrates by means of surface crosslinking, surface activation, or deposition of adhesion layers can improve the adhesion quality of thin films to these substrates.[7] Plasma pretreatment using Ar or an Ar-N_2 mixture has been shown to improve adhesion of plasma deposits to polymers.[40] All substrates used in this study were plasma pretreated with Ar. It is clear that additional work is required for improving the adhesion quality of the films deposited at low RF power levels.

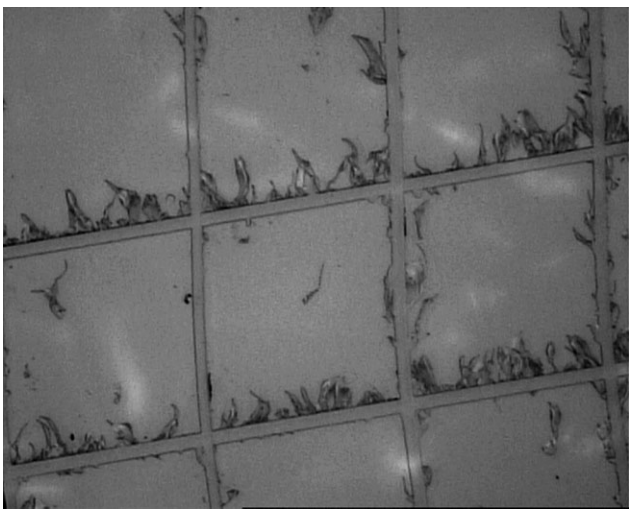

Figure 11 Sample 3 deposited at 25 W on glass (example of crosshatch rating of 2). Crosshatch represents 1 × 1 mm.

The optical images obtained for the 10-W samples suggest a difference in the hardness of these samples in comparison with the films deposited at higher RF power levels. For the thin films deposited at an RF power of 25 W or higher, the areas that were not affected by the tape test appear uniform (Figs. 10 and 11); however, for the 10 W samples (Fig. 13), a significant amount of deformation, in addition to adhesion failing, occurred to the sample on applying and subsequent removal of the tape. An increase in hardness for an increase in RF power has been reported previously for plasma polymers.[39,41,42] This

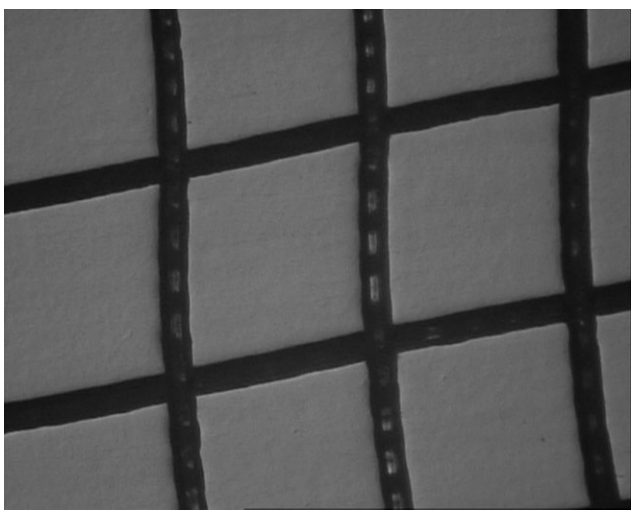

Figure 10 Sample 3 deposited at 75 W on PS (example of crosshatch rating of 5). Cross hatch represents 1 × 1 mm.

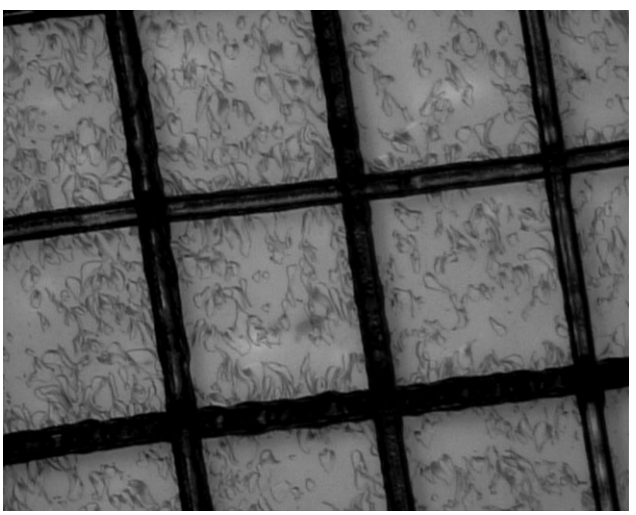

Figure 12 Sample 2 deposited at 25 W on PET (example of crosshatch rating of 0). Crosshatch represents 1 × 1 mm.

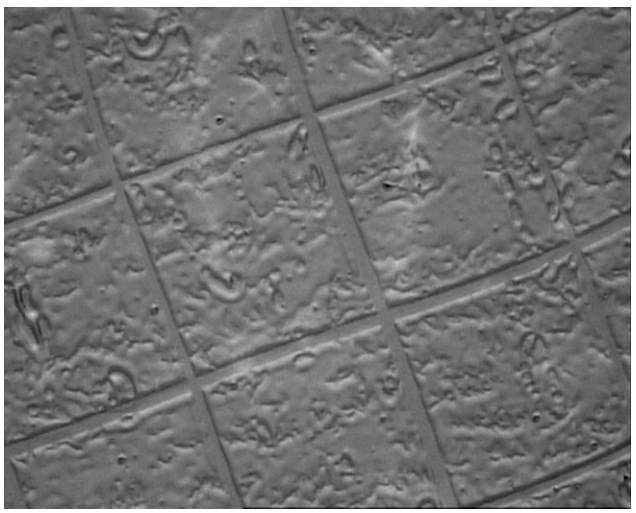

Figure 13 Sample 1 deposited at 10 W on glass (example of crosshatch rating of 0). Crosshatch represents 1 × 1 mm.

trend is typically attributed to an increase in cross-link density associated with increasing applied RF power and would account for the apparent change in hardness observed.

It was evident from the experimental data that there was some variation in the quality of adhesion within sample groups. The crosshatch tape adhesion test provides a qualitative result for adhesion, and as such the accuracy of the test is dependent on correctly identifying the degree of delamination from optical images. A difference of approximately 5% between samples can potentially result in a difference in ratings. As such, there is a limitation as to the usefulness of such a test and should be used as an approximate result.

CONCLUSION

Thin films have been fabricated from LAEO using RF plasma polymerization and their solubility and adhesion characteristics determined. CA data have been obtained for the polymer fabricated at four different RF power levels using six solvents. For the 10-W sample, evidence of adsorption of the solvent into the polymer and reorientation of functionalities at the solid–liquid interface was present for all solvents, with the exception of water. For the polymers deposited at high RF power levels, the magnitude at which these reactions occurred decreased, with the exception for ethylene glycol, where the magnitude appeared unchanged with respect to RF power. The CA data were used to determine the surface tension values of the polymers using three approaches; the VCG, EOS, and Fowkes methods. For the VCG and EOS approaches, only surface tension data obtained from water CA values were considered. Results obtained from the VCG and Fowkes approach are believed to represent the polymer more accurately as they require more than one CA value to determine the surface tension. Based on these criteria, surface tension ranges have been established for the polymers fabricated at 10 W (39.53–45.94), 25 W (33.93–36.34), 50 W (34.26–37.63), and 75 W (36.61–38.38). The polymer demonstrated a relatively strong electron–donor component and a negligible electronic acceptor component and was therefore monopolar in nature. Solubility results obtained from interfacial tension values indicate that the polymer would resist solubilization from the solvents examined. However, the dissolution of the 10-W sample in chloroform demonstrated the importance of a stable solvent–solid interface when obtaining CA data. An adhesion study established that for all substrates used, the films deposited at high RF powers provided the best adhesion quality, whereas the films produced at low RF powers adhered poorly to the substrates. This trend was attributed to an improvement in interfacial bonding as a result of the increase in RF power and associated ion bombardment during deposition.

The authors are grateful to the financial support provided under the RIRDC and ARC LIEF and DP schemes. CDE is grateful to the APA and RIRDC scholarships. We are grateful to Ms Ruilan Liu for access to the solvent DMSO and to the Advanced Analytical Centre at JCU for use of the optical microscope.

References

1. Kim, M. C.; Cho, S. H.; Han, J. G.; Hong, B. Y.; Kim, Y. J.; Yang, S. H.; Boo, J. H. Surf Coat Technol 2003, 169, 595.
2. Sajeev, U. S.; Mathai, C. J.; Saravanan, S.; Ashokan, R. R.; Venkatachalam, S.; Anantharaman, M. R. Bull Mater Sci 2006, 29, 159.
3. Shi, F. F. Surf Coat Technol 1996, 82, 1.
4. Muir, B. W.; Thissen, H.; Simon, G. P.; Murphy, P. J.; Griesser, H. J. Thin Solid Films 2006, 500, 34.
5. Sohn, S.; Kim, K.; Kho, S.; Jung, D.; Boo, J. H. J Alloy Compd 2008, 449, 191.
6. Begou, T.; Beche, B.; Goullet, A.; Landesman, J. P.; Granier, A.; Cardinaud, C.; Gaviot, E.; Camberlein, L.; Grossard, N.; Jezequel, G.; Zyss, J. Opt Mater 2007, 30, 657.
7. Forch, R.; Chifen, A. N.; Bousquet, A.; Khor, H. L.; Jungblut, M.; Chu, L. Q.; Zhang, Z.; Osey-Mensah, I.; Sinner, E. K.; Knoll, W. Chem Vapor Depos 2007, 13, 280.
8. Siow, K. S.; Britcher, L.; Kumar, S.; Griesser, H. J. Plasma Processes Polym 2006, 3, 392.
9. Jacob, M. V.; Easton, C. D.; Woods, G. S.; Berndt, C. C. Thin Solid Films 2008, 516, 3884.
10. Easton, C. D.; Jacob, M. V.; Shanks, R. A.; Bowden, B. F. Chem Vapor Depos, to appear.
11. Easton, C. D.; Jacob, M. V. Thin Solid Films 2009, 517, 4402.
12. Easton, C. D.; Jacob, M. V. Polym Degrad Stab 2009, 94, 597.
13. Peterson, L. The Australian Lavender Industry: A Review of Oil Production and Related Products; Rural Industries Research and Development Corporation, Barton, A.C.T.; Australia, 2002.

14. Shellie, R.; Mondello, L.; Marriott, P.; Dugo, G. J Chromatogr A 2002, 970, 225.
15. Li, W. L.; Tegenfeldt, J. O.; Chen, L.; Austin, R. H.; Chou, S. Y.; Kohl, P. A.; Krotine, J.; Sturm, J. C. Nanotechnology 2003, 14, 578.
16. Park, S.; Allen, S. A. B.; Kohl, P. A. J Electron Mater 2008, 37, 1524.
17. Park, S.; Allen, S. A. B.; Kohl, P. A. J Electron Mater 2008, 37, 1534.
18. Gaillard, F.; De Pontcharra, J.; Gosset, L. G.; Lyan, P.; Bouchu, D.; Daamen, R.; Louveau, O.; Besson, P.; Passemard, G.; Torres, J. Microelectron Eng 2006, 83, 2309.
19. Gosset, L. G.; Farcy, A.; De Pontcharra, J.; Lyan, P.; Daamen, R.; Verheijden, G.; Arnal, V.; Gaillard, F.; Bouchu, D.; Bancken, P. H. L.; Vandeweyer, T.; Michelon, J.; Hoang, V. N.; Hoofman, R. M.; Torres, J. Microelectron Eng 2005, 82, 321.
20. Wu, S. H.; Shanks, R. A. J Appl Polym Sci 2004, 93, 1493.
21. Van oss, C. J.; Chaudhury, M. K.; Good, R. J. Adv Colloid Interface Sci 1987, 28, 35.
22. Vanoss, C. J.; Chaudhury, M. K.; Good, R. J. Chem Rev 1988, 88, 927.
23. Tavana, H.; Neumann, A. W. Adv Colloid Interface Sci 2007, 132, 1.
24. Kwok, D. Y.; Neumann, A. W. Adv Colloid Interface Sci 1999, 81, 167.
25. Wu, W.; Giese, R. F.; Vanoss, C. J. Langmuir 1995, 11, 379.
26. Kwok, D. Y.; Li, D.; Neumann, A. W. Langmuir 1994, 10, 1323.
27. Kwok, D. Y.; Lin, R.; Mui, M.; Neumann, A. W. Colloids Surf a-Physicochemical Eng Aspects 1996, 116, 63.
28. Johnson, R. E.; Dettre, R. H. Langmuir 1989, 5, 293.
29. Shalel-Levanon, S.; Marmur, A. J Colloid Interface Sci 2003, 262, 489.
30. Balkenende, A. R.; Van De Boogaard, H.; Scholten, M.; Willard, N. P. Langmuir 1998, 14, 5907.
31. Deshmukh, R. R.; Shetty, A. R. J Appl Polym Sci 2008, 107, 3707.
32. Fowkes, F. M. J Phys Chem 1963, 67, 2538.
33. Vanoss, C. J.; Good, R. J.; Chaudhury, M. K. Langmuir 1988, 4, 884.
34. Yasuda, H. K.; Yu, Q. S.; Reddy, C. M.; Moffitt, C. E.; Wieliczka, D. M. J Appl Polym Sci 2002, 85, 1443.
35. Sedev, R. V.; Petrov, J. G.; Neumann, A. W. J Colloid Interface Sci 1996, 180, 36.
36. Alexander, M. R.; Duc, T. M. Polymer 1999, 40, 5479.
37. Speight, J. A. Lange's Handbook of Chemisty; The McGraw-Hill Companies, Inc.: New York, 2005.
38. Detomaso, L.; Gristina, R.; Senesi, G. S.; D'agostino, R.; Favia, P. Biomaterials 2005, 26, 3831.
39. Cech, V. IEEE Trans Plasma Sci 2006, 34, 1148.
40. Vallon, S.; Hofrichter, A.; Drevillon, B.; Klembergsapieha, J. E.; Martinu, L.; Poncinepaillard, F. Thin Solid Films 1996, 291, 68.
41. Cech, V.; Studynka, J.; Conte, N.; Perina, V. Surf Coat Technol 2007, 201, 5512.
42. Bae, I. S.; Cho, S. J.; Choi, W. S.; Cho, H. J.; Hong, B.; Jeong, H. D.; Boo, J. H. Prog Org Coat 2008, 61, 245.